Machine Learning–Derived Baseline Visual Field Patterns Predict Future Glaucoma Onset in the Ocular Hypertension Treatment Study

Rishabh K. Singh,[1,2] Sophie Smith,[3] John Fingert,[4] Mae Gordon,[5] Michael Kass,[5] Todd Scheetz,[4] Ayellet V. Segrè,[6,7] Janey Wiggs,[6,7] Tobias Elze,[2] and Nazlee Zebardast[6]

[1]Department of Ophthalmology, Columbia University Medical Center, New York, New York, United States
[2]Schepens Eye Research Institute, Harvard Medical School, Boston, Massachusetts, United States
[3]Tufts University School of Medicine, Boston, Massachusetts, United States
[4]Carver College of Medicine, University of Iowa, Iowa City, Iowa, United States
[5]Washington University School of Medicine, St. Louis, Missouri, United States
[6]Massachusetts Eye and Ear, Harvard Medical School, Boston, Massachusetts, United States
[7]Ocular Genomics Institute, Massachusetts Eye and Ear, Boston, Massachusetts, United States

Correspondence: Nazlee Zebardast, Massachusetts Eye and Ear, Harvard Medical School, 243 Charles Street, Boston, MA 02114, USA; nazlee_zebardast@meei.harvard.edu.

NZ and TE are joint senior authors.

Received: August 6, 2023
Accepted: February 5, 2024
Published: February 23, 2024

Citation: Singh RK, Smith S, Fingert J, et al. Machine learning–derived baseline visual field patterns predict future glaucoma onset in the ocular hypertension treatment study. *Invest Ophthalmol Vis Sci.* 2024;65(2):35. https://doi.org/10.1167/iovs.65.2.35

Purpose. The Ocular Hypertension Treatment Study (OHTS) identified risk factors for primary open-angle glaucoma (POAG) in patients with ocular hypertension, including pattern standard deviation (PSD). Archetypal analysis, an unsupervised machine learning method, may offer a more interpretable approach to risk stratification by identifying patterns in baseline visual fields (VFs).

Methods. There were 3272 eyes available in the OHTS. Archetypal analysis was applied using 24-2 baseline VFs, and model selection was performed with cross-validation. Decomposition coefficients for archetypes (ATs) were calculated. A penalized Cox proportional hazards model was implemented to select discriminative ATs. The AT model was compared to the OHTS model. Associations were identified between ATs with both POAG onset and VF progression, defined by mean deviation change per year.

Results. We selected 8494 baseline VFs. Optimal AT count was 19. The highest prevalence ATs were AT9, AT11, and AT7. The AT-based prediction model had a C-index of 0.75 for POAG onset. Multivariable models demonstrated that a one-interquartile range increase in the AT5 (hazard ratio [HR] = 1.14; 95% confidence interval [CI], 1.04–1.25), AT8 (HR = 1.22; 95% CI, 1.09–1.37), AT15 (HR = 1.26; 95% CI, 1.12–1.41), and AT17 (HR = 1.17; 95% CI, 1.03–1.31) coefficients conferred increased risk of POAG onset. AT5, AT10, and AT14 were significantly associated with rapid VF progression. In a subgroup analysis by high-risk ATs (>95th percentile or <75th percentile coefficients), PSD lost significance as a predictor of POAG in the low-risk group.

Conclusions. Baseline VFs, prior to detectable glaucomatous damage, contain occult patterns representing early changes that may increase the risk of POAG onset and VF progression in patients with ocular hypertension. The relationship between PSD and POAG is modified by the presence of high-risk patterns at baseline. An AT-based prediction model for POAG may provide more interpretable glaucoma-specific information in a clinical setting.

Keywords: glaucoma, ocular hypertension, risk stratification, visual field, archetypal analysis

Glaucoma is the leading cause of irreversible blindness worldwide. Primary open-angle glaucoma (POAG) accounts for nearly 69% of the global prevalence.[1] Identification of high-risk patients at an early stage is necessary for the prevention of glaucomatous vision loss.[2] To date, intraocular pressure (IOP) remains the only modifiable risk factor for the development and progression of POAG. The Ocular Hypertension Treatment Study (OHTS) was a landmark trial that determined that early treatment with topical IOP-lowering therapy may reduce POAG incidence in patients with ocular hypertension.[3] It also led to the creation of a prediction model that includes age, IOP, central corneal thickness (CCT), vertical cup-disc ratio (VCDR), and visual field (VF) pattern standard deviation (PSD) for POAG risk stratification.

Routine VF testing with standard automated perimetry is standard of care for the diagnosis and monitoring of POAG. PSD is a summary statistic that measures nonuniformity in a VF, with high values for severe focal defects and low values for uniformly normal or severely damaged

fields.[4] In the OHTS, a higher baseline PSD was found to be predictive of future POAG onset. This finding was replicated in the Diagnostic Innovations in Glaucoma Study (DIGS) and European Glaucoma Prevention Study (EGPS) cohorts.[5,6] Although the PSD values used in the OHTS baseline prediction model were within normal limits, the possibility remains that higher PSD may have represented early but clinically non-discernible glaucomatous damage.[7] The question remains whether occult patterns are present in baseline VFs, defined as non-glaucomatous by the OHTS Endpoint Committee, and, if so, whether these patterns may predict future POAG onset.

Archetypal analysis (AA), an unsupervised machine-learning method, offers an approach to identify interpretable component patterns from heterogeneous VF datasets.[8] Unsupervised machine-learning methods are less prone to bias than qualitative classification systems, as they apply no prior knowledge about glaucomatous changes.[8] Existing applications of machine learning to VFs primarily aim to diagnose glaucoma or identify disease progression.[9–13] Prediction of future disease onset is a more challenging problem, as signs of early disease are less likely to be discernible and requires a robust longitudinal dataset such as the OHTS.

Prior studies applying AA to VFs have shown that AA is a robust method for identification of clinically interpretable patterns in VFs from patients with known POAG.[8,13,14] AA may additionally enable identification of relevant VF patterns at a preclinical stage of disease. If a VF with high PSD in a patient with ocular hypertension can be categorized into subtypes, it may be used more precisely for POAG risk stratification. Perhaps some types of non-uniformity may be normal physiologic variants while others represent early occult glaucomatous changes. In this study, we applied AA to the OHTS to identify baseline VF patterns that may indicate increased risk for glaucoma onset.

Methods

OHTS Background

This study was a secondary analysis of data from the OHTS, which was a randomized clinical trial assessing the safety and efficacy of early treatment with topical IOP-lowering therapy among patients with ocular hypertension. This study was exempt from institutional review board approval as we used only deidentified data. All methods adhered to the tenets of the Declaration of Helsinki for research involving human participants.

The OHTS recruited 1636 participants with ocular hypertension from 22 sites. Prior to randomization, each participant was required to have a Humphrey VF and optic nerve head (ONH) photograph with no detectable signs of glaucomatous damage. Randomization of participants to observation began in 1994 and ended in 1996. Participants were followed with Humphrey VF testing semiannually and ONH photography annually until the completion of phase 1 in June 2002. After each 12-month follow-up visit, the Optic Disc Photography Reading Center compared the baseline test with the most recent test in a masked fashion in order to identify evidence of disc changes. The Visual Field Reading Center classified a reliable VF as abnormal if the glaucoma hemifield test (GHT) was outside of normal limits and/or the corrected pattern standard deviation was $P < 5\%$.[7] Three consecutive abnormal VFs were required due to a high percentage of normal VFs appearing after the first abnormal VF.[7] The Endpoint Committee determined if the cause of changes was due to POAG based on a review of the clinical history. Phase 2 of the OHTS began in June 2002 and continued until March 2009. During this phase, all participants, including the phase 1 observation group, received topical IOP-lowering therapy. Phase 3 of the OHTS, which began in July 2015 and continued until June 2020, assessed the cumulative incidence of POAG over 20 years of follow-up. Data analysis in this study was limited to 20 years of follow-up per participant.

Archetypal Analysis

AA is a matrix factorization method that decomposes data into a *linear* combination of representative patterns, or archetypes (ATs).[15] Compared to component approaches, AA does not require data to fall onto axes or follow certain distributions. Compared to cluster analysis methods, ATs lie on the edges of the data space as opposed to the centers, resulting in more interpretable and distinctive glaucomatous VF loss patterns.[8] In the OHTS, 3272 eyes from 1636 participants were available. Up to three baseline VFs were selected per eye, including two pre-randomization in the OHTS and one 6 months after randomization. At the 6-month timepoint, no OHTS participants had developed signs of glaucomatous VF change, as defined by the Endpoint Committee. Inclusion of the 6-month time point enables the use of a larger AA training set, as VFs are a modality prone to high variability and noise.

The 30-2 VF sensitivity values were spatially mapped to an equivalent 24-2 field and converted to total deviation values using normative data. The AA was trained using baseline fields with minimization of reconstruction error via residual sum of squares (RSS) for the selection of the optimal AT count (k), with the AT library on an R 4.2.2 platform (R Foundation for Statistical Computing, Vienna, Austria). For each k between 5 and 30, 10-fold cross-validation (CV) was performed and the mean RSS was determined for model selection. AT decomposition coefficients were calculated for all VFs. Decomposition coefficients represent the strength of contribution of the AT to the final VF. The original VF can then be reconstructed from the k-dimensional space by calculating a weighted sum of the ATs and their respective decomposition coefficients. Selected baseline fields used for training were averaged into a single aggregate baseline field by calculating the mean of each decomposition coefficient by AT.

Baseline Prediction Models

Survival analysis was performed to predict the time to POAG onset and to assess factors influencing the conversion of ocular hypertension to POAG. Cox proportional hazard (Cox-PH) models were implemented with the scikit-survival 0.19.0 and lifelines 0.27.4 libraries on a Python 3.9.12 platform.[16,17] A reference Cox-PH model representing the five-factor OHTS model was first developed, with OHTS baseline covariates (age, IOP, VCDR, PSD, and CCT), as well as randomization status (RS). RS was included in all models to control for the effect of delayed treatment on POAG onset in OHTS phase 1 participants.

Investigative Ophthalmology & Visual Science

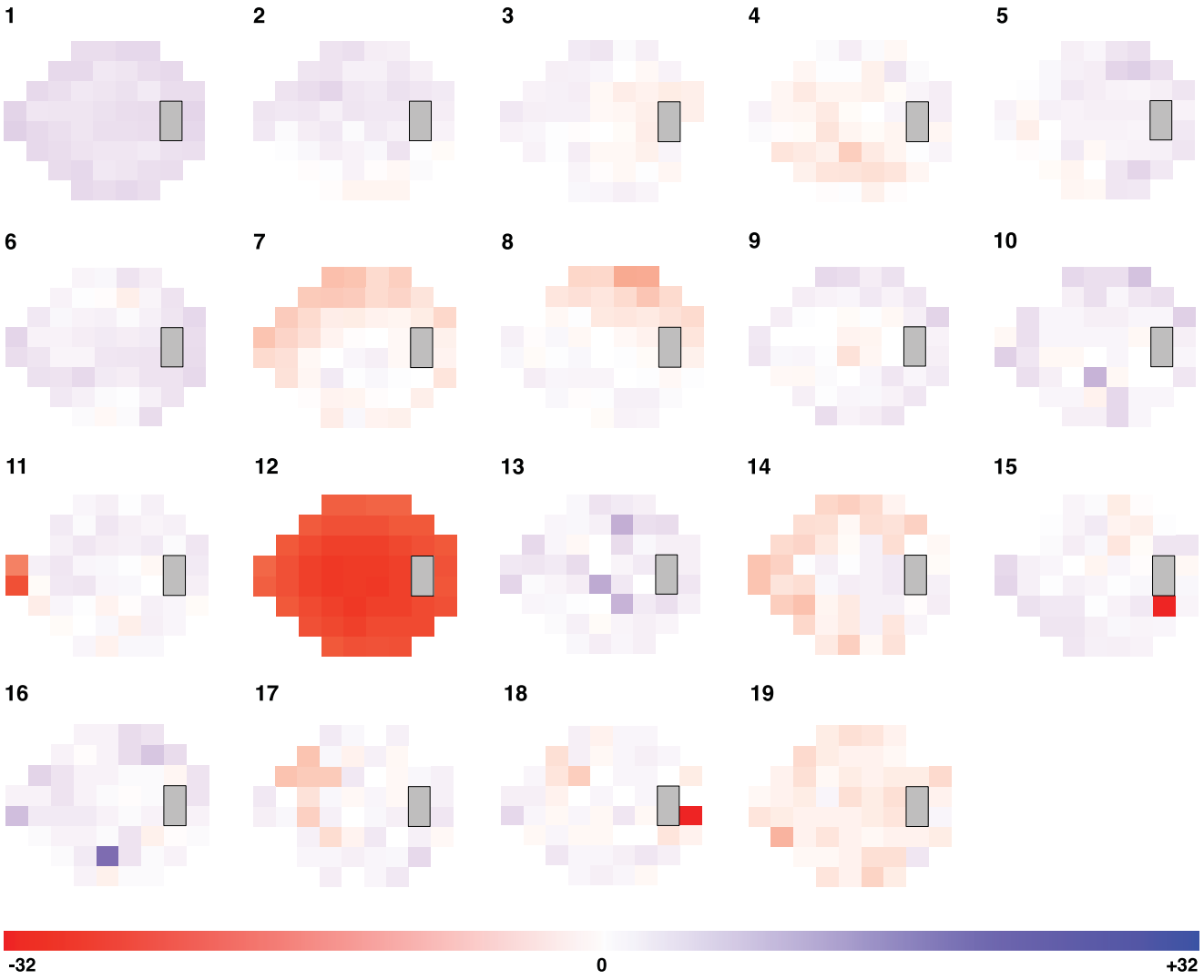

Figure 1. Identified VF patterns. *Orange regions* represent regions of relative loss. *Blue regions* represent regions of relative preservation within the field.

To develop a new model using baseline ATs, a penalized Cox-PH model was implemented to select the most discriminative VF features. As high collinearity and dimensionality are present in a model containing 19 ATs, penalization approaches may improve discriminative feature selection.[18,19] Elastic net penalization was chosen, as it combines subset selection properties from least absolute shrinkage and selection operator (LASSO) regression and regularization from ridge regression approaches.[19] When a high degree of collinearity may be present, as in the case of AT decomposition coefficients that sum to 1, LASSO regression may randomly select a subset feature/AT. Ridge regression, on the other hand, performs effective shrinkage of regression coefficients but does not perform feature selection. From an initial set of 23 covariates (age, IOP, VCDR, CCT, RS, and 19 AT decomposition coefficients), the best L1 ratio, α, and a subset of discriminative features were selected using 10-fold CV. The L1 ratio represents the balance between LASSO and ridge regression penalties in elastic net regression; α is a weight that represents the amount of coefficient shrinkage in the LASSO component of the regression and ultimately determines the number of final subset features. PSD was excluded in feature selection as a collinear measure of localized VF change.

Statistical Analysis

Predictive performance of the reference OHTS model and AT-based model were compared using concordance index (C-index) and log-likelihood ratio. The mean C-index and log-likelihood ratio were calculated across 10-folds of cross-validation, and 95% confidence intervals (CIs) were additionally provided. Group shuffling splitting was applied to generate CV train–test sets, such that both eyes from the same patient were selected into the same set. Cumulative/dynamic receiver operating characteristic (ROC) curve–area under the ROC curve (AUC_t) scores were additionally plotted, as sensitivity and specificity of survival regression models vary with time.[20–22] AUC_t assesses the ability of the model to distinguish cumulative cases (who experienced an event by each time point) from dynamic controls. AUC_t was calculated in 0.5-year intervals. Hazard ratios (HRs) and 95% CIs were calculated for each discriminative AT selected by penalized regression. HRs were calculated using simplified

Cox-PH models with a single AT coefficient and the same covariates as the penalized model (age, IOP, VCDR, CCT, RS). Decomposition coefficients were transformed using robust scaling, centered at 0 with an interquartile range of 1. Robust scaling was chosen over standard scaling for decreased sensitivity to outliers in AT distributions. Given the high number of comparisons made, increasing the likelihood of erroneous inferences, false discovery rate correction was performed with *P* values. We additionally performed sensitivity analyses using differing Endpoint Committee diagnosis modalities: VF only, fundus photograph only, and both VF and fundus photograph (Supplementary Material S1).

In order to provide an alternate modality for identification of VF progression (independent from the GHT used by the Endpoint Committee), a secondary analysis was completed. VF progression was defined by the mean deviation (MD) change per year (<−0.5 dB/y) over the follow-up period.[23] Logistic regression was performed with inputs of each AT coefficient and adjustment for age, IOP, VCDR, CCT, and RS. Odds ratios (ORs) and 95% CIs were calculated.

The relationship between the predictive power of PSD and component patterns was additionally evaluated using Cox-PH models with high-risk AT and low-risk AT subgroups of eyes. The high-risk AT group was defined by having any decomposition coefficient exceeding the 95th percentile among the ATs identified to be significant predictors of POAG onset. The low-risk AT group was defined by having decomposition coefficients below the 75th percentile in ATs identified to be significant predictors of POAG onset. HRs and 95% CIs for PSD were calculated for both the high-risk AT and low-risk AT subgroups of eyes.

For patterns identified as being significantly associated with POAG onset, baseline characteristics were compared within the OHTS cohort. Categorical baseline characteristics were compared with χ^2 tests, and continuous variables were compared with two-sample *t*-tests.

Results

The 8494 baseline VFs that were selected had an average MD of 0.07 ± 1.50. Optimal AT count was 19 (RSS = 0.085), and the identified VF patterns are shown in Figure 1. Proportions of fields with each AT as the predominant component pattern (by highest decomposition coefficient) are shown in Figure 2A. Mean decomposition coefficients are shown in Figure 2B. Patterns 9, 11, and 7 were the most prevalent with both metrics.

In penalized regression, 17 covariates were selected in the best performing model (in order of highest coefficient to lowest): VCDR, IOP, age, CCT, randomization status, AT8, AT15, AT9, AT17, AT14, AT5, AT11, AT19, AT10, AT3, AT12, and AT18. The reference OHTS model with PSD has a C-index of 0.74 (95% CI, 0.67–0.82) and log-likelihood ratio of 295.34 (95% CI, 264.21–326.48) for the prediction of POAG onset. The new model with penalization-selected ATs replacing PSD has a C-index of 0.75 (95% CI, 0.68–0.83) and log-likelihood ratio of 325.20 (95% CI, 293.71–356.68) (Fig. 3). A third model applying both ATs and PSD has a C-index of 0.75 (95% CI, 0.68–0.92) and log-likelihood ratio of 331.67 (95% CI, 300.19–363.16).

Sensitivity analyses using VF-based, fundus photography–based, and bimodal POAG diagnosis outcomes are shown in Supplementary Material S1. Both the PSD model, with a C-index of 0.72 (95% CI, 0.57–0.86), and the AT model, with a C-index of 0.71 (95% CI, 0.57–0.85), had the lowest performance using fundus-photography–based outcomes (Supplementary Material S1A). Both models performed best with bimodal outcomes. The PSD model produced a C-index of 0.80 (95% CI, 0.70–0.90), and the AT model produced a C-index of 0.80 (95% CI, 0.69–0.91) (Supplementary Material S1C).

ATs selected by the penalized Cox model were analyzed in univariate and multivariable models to assess HRs. In univariate models, AT5, AT8, AT10, AT15, and AT17 indicated

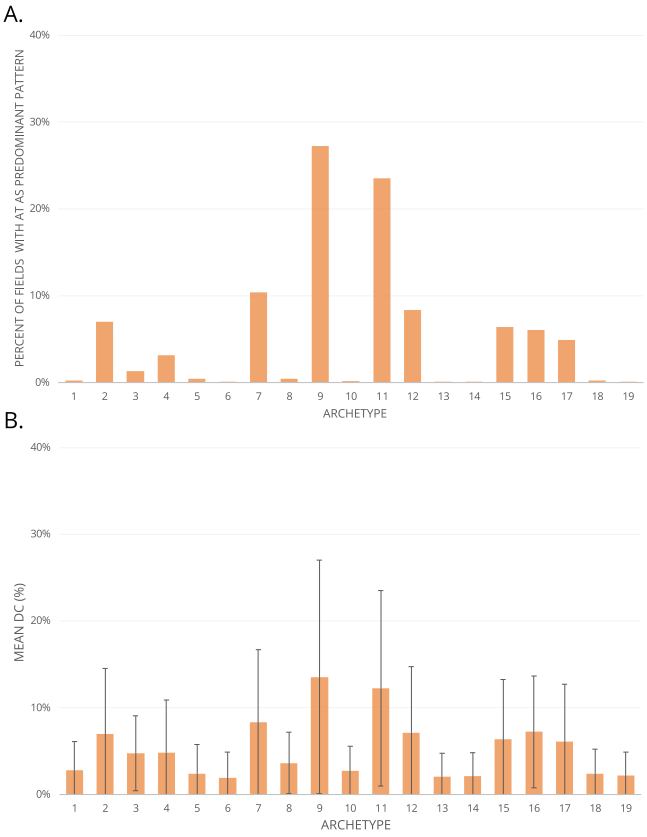

Figure 2. For each AT, the percentage of VFs in which an AT is the most prevalent decomposition pattern is shown (**A**), as well as the mean decomposition coefficient (**B**).

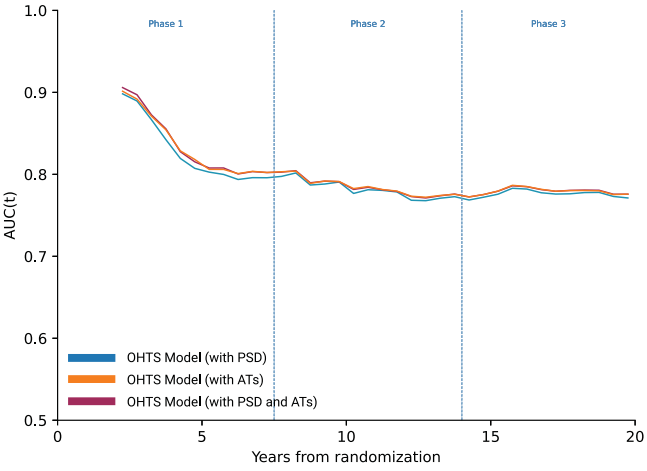

Figure 3. AUC_t curves for baseline prediction models, calculated in 0.5-year intervals.

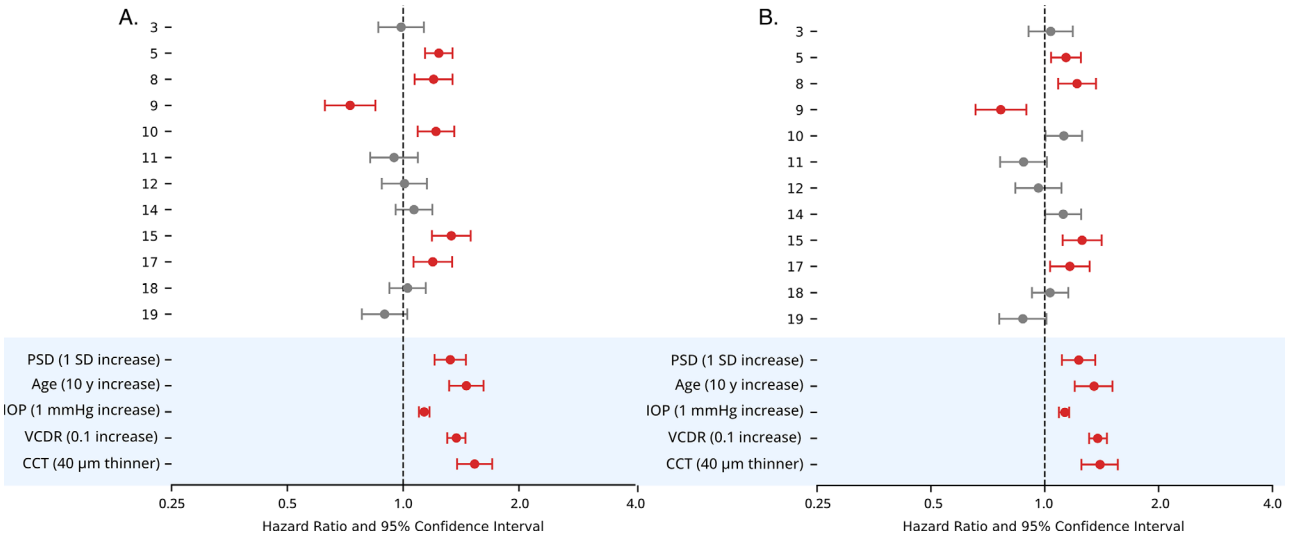

Figure 4. Cox-PH HRs and 95% CIs. *Red-shaded intervals* represent $P < 0.05$ after false discovery rate correction. Variables under *blue shading* show HRs for reference from the OHTS baseline model. (**A**) Univariate HRs. (**B**) Multivariable HRs.

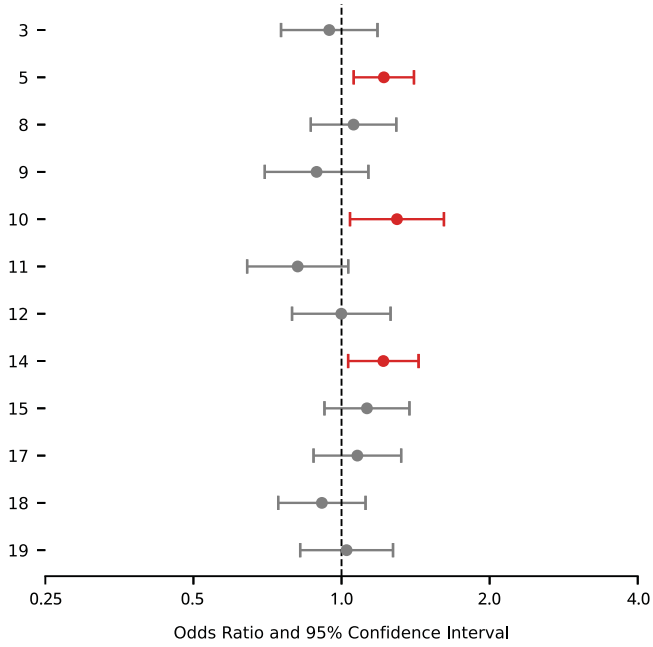

Figure 5. Multivariable ORs and 95% CIs for relationship between AT coefficients and rapid VF progression. *Red-shaded intervals* represent $P < 0.05$ after false discovery rate correction.

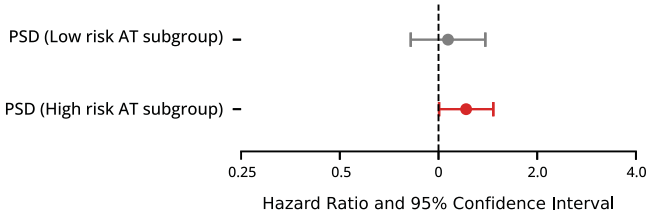

Figure 6. Multivariable HRs and 95% CIs for PSD as a predictor of POAG onset, in subgroups defined by low- and high-risk AT coefficients. *Red-shaded intervals* represent $P < 0.05$.

an increased hazard for POAG onset, whereas AT9 indicated a decreased hazard (Fig. 4A). In multivariable regression models adjusted for age, IOP, VCDR, CCT, and randomization status, AT5, AT8, AT15, and AT17 were associated with increased hazard for POAG onset, and AT9 indicated a decreased hazard (Fig. 4B). AT10 was no longer significant in multivariable analysis.

In secondary analysis of POAG endpoint defined by rate of VF progression, 161 eyes met the criteria for rapid VF progression (<−0.5 dB/y change in MD). We found that one of the ATs predictive of POAG onset was additionally associated with rapid VF progression (Fig. 5). AT10, which only reached significance for POAG onset in univariate analysis, was additionally associated with rapid VF progression (Fig. 5). An additional AT that did not reach significance in the primary analysis, AT14, was associated with rapid VF progression (Fig. 5).

In subgroup analysis stratified by AT risk levels (using AT5, AT8, AT15, and AT17 from the multivariable analysis), the high-risk AT subgroup contained 735 eyes (22%) with a mean PSD of 2.01 ± 0.25 dB. The low-risk AT subgroup contained 883 eyes (27%) with a mean PSD of 1.86 ± 0.23 dB. In the high-risk AT group, PSD remained a significant predictor of POAG onset (HR = 1.21; 95% CI, 1.00–1.47), with a HR comparable to our primary analysis in the entire OHTS cohort (HR = 1.23; 95% CI, 1.11–1.36) (Fig. 6). In the low-risk AT group, PSD lost significance as a predictor of POAG onset (HR = 1.07; 95% CI, 0.82–1.39) (Fig. 6).

For ATs found to have significant HRs, subsets of participants with high AT quartiles are compared to the entire OHTS population in the Table. The top AT5 and AT15 quartiles had significantly higher mean ages than the entire OHTS cohort. The top AT5, AT8, and AT15 quartiles had a higher proportion of self-reported Black race participants than the entire OHTS cohort. The top AT5, AT15, and AT17 quartiles had significantly thinner CCT values than the entire OHTS cohort. The top AT5, AT15, and AT17 quartiles had significantly higher PSDs than the entire OHTS cohort. AT9 showed opposite trends, with significantly lower age and

Investigative Ophthalmology & Visual Science

Table. Description of Characteristics of Participants in Top Quartile for AT5, AT8, AT9, AT15, and AT17 Decomposition Coefficients

		Top Quartile				
	Entire OHTS Cohort	**AT5**	**AT8**	**AT9**	**AT15**	**AT17**
Age (y)	56.04	57.37*	55.62	54.96*	56.97*	56.27
Male sex (%)	43.10	43.92	38.63*	44.13	40.95	48.76*
African American (%)	24.87	34.66*	28.48*	19.80*	34.96*	23.75
VCDR	0.39	0.41	0.38	0.40	0.40	0.39
CCT (µm)	572.75	567.23*	572.50	573.20	567.02*	569.26*
IOP (mmHg)	24.93	25.13	24.85	24.71	25.03	24.85
PSD (dB)	1.91	1.95*	1.93	1.84*	1.98*	1.96*
20-year POAG conversion (%)	12.22	17.40*	14.67*	10.02*	16.66*	16.29*

* Denotes statically significant difference compared to the full OHTS cohort ($P < 0.05$).

fewer self-reported Black participants than the entire OHTS population.

Discussion

We showed that baseline VFs in the OHTS cohort may contain information predictive of future POAG onset. Using AA, we identified 19 component patterns in baseline fields, found that an AT-based prediction model performs at least as well as the existing PSD-based one, and observed that decomposition coefficients for five patterns are associated with POAG onset. Importantly, we identified baseline patterns associated with rapid VF progression and found that the association between PSD and POAG is dependent on the presence of high-risk component patterns at baseline.

When VF patterns are identified in clinically non-glaucomatous eyes, a key question is whether the patterns represent a preclinical stage of disease or normal variation. Some of our baseline VF patterns appear to correspond to known POAG VF abnormalities previously reported in the OHTS.[24] This is a surprising but important result, as these eyes considered to be clinically healthy may otherwise be expected to show non-specific noisy patterns or factorization artifacts. The ability of AA to decompose a field into a weighted sum of patterns appears to enable identification of preclinical patterns that may not be obvious to the clinician's eye. For example, AT8 may represent signs of early superior altitudinal VF loss. AT15 and AT17 resemble partial superior arcuate patterns. AT2, AT5, and AT10 may represent occult partial inferior arcuate defects or early inferior altitudinal changes. AT14 and AT17 may represent early peripheral rim changes; AT9, paracentral changes; AT11, nasal step defect; and AT4, AT12, AT18, and AT19, widespread loss. Paracentral, partial arcuate, and nasal step defects are clinical classifications that have been associated with early glaucomatous damage.[20] Other identified patterns do not appear to clearly correspond to known clinical patterns, such as AT6, AT13, and AT16. These may be factorization artifacts from AA or represent normal variation.

In our application of penalized regression to select for ATs with the strongest associations with POAG onset, our model retained 12 out of 19 loss patterns. When we compared this new AT-based model to the traditional OHTS model that uses PSD as the measure of VF non-uniformity, we found a comparable overall prediction of POAG onset. Our supplementary sensitivity analysis showed that the AT model performed at least as well as the PSD model regardless of POAG diagnosis modality. The strength of the AT model is that it is unlikely to be biased by the reliance of the OHTS Endpoint Committee on the GHT to identify glaucomatous VF changes. Although the improvements in the OHTS model from the usage of ATs are small, they may provide more detailed information to a clinician about loss subtypes than high PSD alone. The similarities between AA-derived VF patterns and known POAG VF abnormalities suggest that our machine learning (ML) method may identify occult glaucomatous loss. This is further supported by our finding that the effect sizes of each AT are comparable in magnitude to those of PSD. We also found that the relationship between PSD and POAG risk is modified by the presence of high-risk ATs in baseline VFs. This would suggest that the predictive power of PSD is not due to general non-uniformity alone but rather its ability to capture specific types of preclinical loss. PSD may be less clinically relevant when only non-specific patterns are prevalent in a VF. A combination model containing both PSD and ATs performed almost identically to the AT model, further illustrating how both modalities of representing VF variance largely capture the same information. Unfortunately, due to the date of study initiation, the OHTS does not include baseline structural optical coherence tomography (OCT) data. Correlation of early functional changes to structural degradation in future studies may further support risk stratification efforts.

Of the ATs found to significantly increase the risk for POAG, three (AT8, AT15, and AT17) may represent occult superior loss patterns. One (AT5) may represent early inferior loss. In our secondary analysis, an additional inferior loss pattern (AT10) and a pattern resembling early peripheral rim changes (AT14) were additionally found to be associated with faster VF progression. Pattern AT9, possibly representing cecocentral loss, appears to correlate with decreased incidence of POAG. Prior studies have found that, in early POAG, when VF defects are localized to a single hemifield, the superior hemifield is the most frequently affected.[25,26] Given the well-established pattern of inferior neuroretinal rim involvement in glaucoma, inferior retinal nerve fiber layer quadrants also tend to undergo the greatest amount of thinning.[24,27] It is possible that preclinical VF changes observed here may correlate with structural changes that would have been observed on OCT. Although OCT was not available at the time of the OHTS, the prevalence of early superior loss patterns suggests that many included participants may have had preclinical levels of inferior retinal nerve fiber layer thinning present. A faster rate of VF loss in the superior hemifield compared to the inferior hemifield has also been observed in POAG.[26] Although it is possible that a higher prevalence of superior hemifield defects may contribute to apparent associations with

Investigative Ophthalmology & Visual Science

POAG risk, we also find that an inferior pattern confers similar risk. The cecocentral pattern may represent a subset of patients with other explanations for occult VF loss, such as macular comorbidities. Although the OHTS excluded patients with some comorbidities that cause central VF loss, other confounding factors such as undiagnosed or preclinical macular disease, or testing noise may have been difficult to exclude. Furthermore, AT patterns are component patterns, and central VF changes may not have been identifiable based on clinical assessment of entire baseline fields. Central VF involvement in glaucoma is more common in later stages of disease and would not be expected to play a role preclinically.[25] Although we cannot make definitive conclusions here due to the lack of detailed ON structural data, our results point to the utility of AT analysis for identifying subtle preclinical changes in VF sensitivity that are predictive of future functional vision loss. Such changes may provide stand-alone information for prognostication or be used to inform the structural–functional correlation that is necessary to identify early glaucoma.

We compared baseline characteristics of participants who had decomposition coefficients in the highest quartiles for AT5, AT8, AT9, AT15, and AT17 and found associations with known OHTS-identified risk factors. Participants with high AT9, associated with decreased POAG risk, were found to be younger and to have lower PSDs compared to the entire OHTS cohort. High AT5, AT8, AT15, and AT17 coefficients were associated with older age, higher proportion of Black race, thinner CCT, or higher PSD. The relative correspondence of these patterns to known risk factors indicates that preclinical signs of disease in VFs are more likely to be present in patients with known higher baseline risk factors.

Clinical application of algorithms applying AA will require validation in a larger and more diverse longitudinal dataset of ocular hypertensive or glaucoma-suspect patients. Additional studies will also likely be needed to identify preclinical patterns in other disease subtypes such as normal-tension glaucoma. This is required to develop normative databases of decomposition coefficients for component patterns. An advantage of traditional AA over the newer nonlinear deep archetypal analysis is model explainability as a linear combination of component patterns.[14,28,29] This may ease interpretation of how decomposition coefficients change over time during monitoring of disease progression. Integration into clinical VF software reports may enable a clinician to identify patients who have high proportions of high-risk patterns outside of normal limits. Another possible advantage of AA is the identification of underlying high-risk patterns in otherwise unreliable or noisy VFs with falsely elevated summary statistics such as PSD. Further correlation to rapid disease progression, underlying genetic risk, and treatment response may further improve the clinical utility of VF decomposition algorithms.

Limitations of this study include limited applicability to patients who do not have elevated baseline IOP or do not match the demographic makeup of OHTS participants. The OHTS focus on ocular hypertension may have also selected for patients who are more likely to have forms of preclinical glaucoma at baseline. Other glaucoma subtypes, such as normal-tension glaucoma, may be associated with different patterns at preclinical stages. Future longitudinal studies in more diverse patient populations may enable identification of more generalizable ATs and corresponding POAG risk. Furthermore, POAG diagnosis by VF in the OHTS was largely defined by abnormal GHTs. The ATs identified as being high risk may be most associated with typical defects captured by the GHT. Finally, VFs are a noisy testing modality, and correlation of baseline patterns to structural data from fundus photography or OCT may produce more robust prediction models.

Conclusions

Baseline VFs, prior to detectable glaucomatous damage, contain occult patterns representing early changes that may increase the risk of future POAG onset in patients with ocular hypertension. The relationship between PSD and POAG is modified by the presence of high-risk patterns at baseline. An archetype-based prediction model for POAG performs at least as well as an existing PSD-based model and may provide more detailed and glaucoma-specific information.

Acknowledgments

Supported by grants from the National Eye Institute, National Institutes of Health (NEI K23EY032634, NEI R01EY032559), Research to Prevent Blindness Career Development Award, American Glaucoma Society Clinician Scientist Award, and The Glaucoma Foundation (NYC). The sponsors or funding organizations had no role in the design or conduct of this research.

Disclosure: **R.K. Singh**, None; **S. Smith**, None; **J. Fingert**, None; **M. Gordon**, None; **M. Kass**, None; **T. Scheetz**, None; **A.V. Segrè**, None; **J. Wiggs**, None; **T. Elze**, None; **N. Zebardast**, None

References

1. Tham YC, Li X, Wong TY, Quigley HA, Aung T, Cheng CY. Global prevalence of glaucoma and projections of glaucoma burden through 2040. *Ophthalmology*. 2014;121(11):2081–2090.
2. Johnson DH. Progress in glaucoma: early detection, new treatments, less blindness. *Ophthalmology*. 2003;110(4):634–635.
3. Kass MA, Heuer DK, Higginbotham EJ, et al. The Ocular Hypertension Treatment Study: a randomized trial determines that topical ocular hypotensive medication delays or prevents the onset of primary open-angle glaucoma. *Arch Ophthalmol*. 2002;120(6):701–713.
4. Yaqub M. Visual fields interpretation in glaucoma: a focus on static automated perimetry. *Community Eye Health*. 2012;25(79-80):1–8.
5. Medeiros FA, Weinreb RN, Sample PA, et al. Validation of a predictive model to estimate the risk of conversion from ocular hypertension to glaucoma. *Arch Ophthalmol*. 2005;123(10):1351–1360.
6. Ocular Hypertension Treatment Study Group, European Glaucoma Prevention Study Group,Gordon MO, et al. Validated prediction model for the development of primary open-angle glaucoma in individuals with ocular hypertension. *Ophthalmology*. 2007;114(1):10–19.
7. Keltner JL, Johnson CA, Quigg JM, Cello KE, Kass MA, Gordon MO. Confirmation of visual field abnormalities in the Ocular Hypertension Treatment Study. Ocular Hypertension Treatment Study Group. *Arch Ophthalmol*. 2000;118(9):1187–1194.
8. Elze T, Pasquale LR, Shen LQ, Chen TC, Wiggs JL, Bex PJ. Patterns of functional vision loss in glaucoma determined with archetypal analysis. *J R Soc Interface*. 2015;12(103):20141118.

9. Wang M, Shen LQ, Pasquale LR, et al. An artificial intelligence approach to detect visual field progression in glaucoma based on spatial pattern analysis. *Invest Ophthalmol Vis Sci*. 2019;60(1):365–375.
10. Yousefi S, Balasubramanian M, Goldbaum MH, et al. Unsupervised Gaussian mixture-model with expectation maximization for detecting glaucomatous progression in standard automated perimetry visual fields. *Transl Vis Sci Technol*. 2016;5(3):2.
11. Yousefi S, Elze T, Pasquale LR, Boland M. Glaucoma monitoring using manifold learning and unsupervised clustering. In: *2018 International Conference on Image and Vision Computing New Zealand (IVCNZ)*. Piscataway, NJ: Institute of Electrical and Electronics Engineers; 2018:1–6.
12. Saeedi O, Boland MV, D'Acunto L, et al. Development and comparison of machine learning algorithms to determine visual field progression. *Transl Vis Sci Technol*. 2021;10(7):27.
13. Wang M, Shen LQ, Pasquale LR, et al. Artificial intelligence classification of central visual field patterns in glaucoma. *Ophthalmology*. 2020;127(6):731–738.
14. Yousefi S, Pasquale LR, Boland MV, Johnson CA. Machine-identified patterns of visual field loss and an association with rapid progression in the Ocular Hypertension Treatment Study. *Ophthalmology*. 2022;129(12):1402–1411.
15. Cutler A, Breiman L. Archetypal analysis. *Technometrics*. 1994;36(4):338–347.
16. Davidson-Pilon C. lifelines: survival analysis in Python. *J Open Source Softw*. 2019;4(40):1317.
17. Pölsterl S. scikit-survival: a library for time-to-event analysis built on top of scikit-learn. *J Mach Learn Res*. 2020;21(212):1–6.
18. Mansiaux Y, Carrat F. Detection of independent associations in a large epidemiologic dataset: a comparison of random forests, boosted regression trees, conventional and penalized logistic regression for identifying independent factors associated with H1N1pdm influenza infections. *BMC Med Res Methodol*. 2014;14(1):99.
19. Simon N, Friedman J, Hastie T, Tibshirani R. Regularization paths for Cox's proportional hazards model via coordinate descent. *J Stat Softw*. 2011;39(5):1–13.
20. Kamarudin AN, Cox T, Kolamunnage-Dona R. Time-dependent ROC curve analysis in medical research: current methods and applications. *BMC Med Res Methodol*. 2017;17(1):53.
21. Heagerty PJ, Lumley T, Pepe MS. Time-dependent ROC curves for censored survival data and a diagnostic marker. *Biometrics*. 2000;56(2):337–344.
22. Lambert J, Chevret S. Summary measure of discrimination in survival models based on cumulative/dynamic time-dependent ROC curves. *Stat Methods Med Res*. 2016;25(5):2088–2102.
23. Chauhan BC, Malik R, Shuba LM, Rafuse PE, Nicolela MT, Artes PH. Rates of glaucomatous visual field change in a large clinical population. *Invest Ophthalmol Vis Sci*. 2014;55(7):4135–4143.
24. Keltner JL. Classification of visual field abnormalities in the Ocular Hypertension Treatment Study. *Arch Ophthalmol*. 2003;121(5):643–650.
25. Germano RAS, Germano CS, Susanna FN, Susanna R. Patterns of visual field loss in early, moderate, and severe stages of open angle glaucoma. *J Glaucoma*. 2022;31(7):609–613.
26. Yousefi S, Sakai H, Murata H, et al. Rates of visual field loss in primary open-angle glaucoma and primary angle-closure glaucoma: asymmetric patterns. *Invest Ophthalmol Vis Sci*. 2018;59(15):5717–5725.
27. Bowd C, Weinreb RN, Williams JM, Zangwill LM. The retinal nerve fiber layer thickness in ocular hypertensive, normal, and glaucomatous eyes with optical coherence tomography. *Arch Ophthalmol*. 2000;118(1):22–26.
28. Thakur A, Rajan P. Deep archetypal analysis based intermediate matching kernel for bioacoustic classification. *IEEE J Sel Top Signal Process*. 2019;13(2):298–309.
29. Keller SM, Samarin M, Arend Torres F, Wieser M, Roth V. Learning extremal representations with deep archetypal analysis. *Int J Comput Vis*. 2021;129(4):805–820.

Investigative Ophthalmology & Visual Science